International Journal of Neural Systems

CONVOLUTIONAL NEURAL NETWORKS-BASED FRAMEWORK FOR EARLY IDENTIFICATION OF DEMENTIA USING MRI OF BRAIN ASYMMETRY

NITSA J HERZOG*
Department of Computer Science, Birkbeck College, University of London, Malet Street London, WC1E 7HZ, UK

GEORGE D MAGOULAS*
Birkbeck Knowledge Lab, Birkbeck College, University of London, Malet Street London, WC1E 7HZ, UK
E-mail: g.magoulas@bbk.ac.uk

Computer-aided diagnosis of health problems and pathological conditions has become a substantial part of medical, biomedical, and computer science research. This article focuses on the diagnosis of early and progressive dementia, building on the potential of deep learning models. The proposed computational framework exploits an MRI brain asymmetry biomarker, which has been associated with early dementia, and employs deep learning architectures for MRI image classification. Identification of early dementia is accomplished by an eight-layered convolutional neural network (CNN) as well as transfer learning of pretrained CNNs from ImageNet. Different instantiations of the proposed CNN architecture are tested. These are equipped with Softmax, SVM, LD or KNN classification layers, assembled as a separate classification module, which are attached to the core CNN architecture. The initial imaging data were obtained from the MRI directory of the ADNI3 database. The independent testing dataset was created using image preprocessing and segmentation algorithms applied to unseen patients' imaging data. The proposed approach demonstrates a 90.12% accuracy in distinguishing patients who are cognitively normal subjects from those who have Alzheimer's Disease (AD), and an 86.40 % accuracy in detecting Early Mild Cognitive Impairment (EMCI).

Keywords: MRI, brain asymmetry, transfer learning, CNN architecture, dementia.

1. Introduction

Computational analysis and modelling of clinical data, imaging methods and machine learning algorithms have led to innovative solutions in several areas of medical diagnosis and in the treatment of neurogenerative diseases [1] [2].

Magnetic Resonance Imaging (MRI) is perhaps the most popular non-invasive imaging method for the diagnosis of brain diseases since it does not use ionizing radiation[2].

This paper focuses on early dementia, or amnestic Mild Cognitive Impairment (aMCI), which is considered a growing problem in public health [3] since 80% of those with aMCI will progress to severe dementia within seven years of initial diagnosis. Structural markers in the MRI images indicate that the patient is at the initial stages of the disease. A noticeable early symptom of dementia is a variation in the symmetry of the brain hemispheres[4] [5], and previous work introduced a method for computing brain asymmetry and investigated the potential and robustness of brain asymmetry features and brain asymmetry images for diagnosis using various machine learning methods. [6]

This article builds on this work to propose a framework that employs the computational method introduced in [6] for generating images of brain asymmetry and includes distinctive architectural configurations of Convolutional Neural Networks (CNNs) for the early detection of dementia. It also extends previous work presented in [7], which concentrated on transfer learning using pretrained Deep Learning (DL) architectures.

* Corresponding author.

In the last 10 years, deep neural networks became the method of choice in intelligent medical diagnosis when images are involved[8]. CNNs belong to this class of methods and allow feature generation and selection through learning, and the various layers of the network play the role of feature extractors generating different types of features. In many cases, this helps in avoiding complicated feature engineering procedures, and when it comes to MRI data it has led to high-performance in medical diagnosis[9].

Transfer learning has been investigated in previous work [7], where a pretrained neural model called AlexNet [10] was used. When transfer learning is adopted, a pretrained model's knowledge is transferred to a new task or even to a new application domain. This can be achieved by adding layers to the pretrained neural networks and selecting a strategy for retraining it using task-related data, such as training only the added layers, retraining the original pretrained network or even retraining the full architecture.[11] There are several examples in the relevant literature where transfer learning has performed better than designing and training a new model from scratch and has significantly reduced the time for training, validation and testing on new tasks without harming generalisation.[12]

In this vein, this work proposes specially created CNN-based models for brain asymmetry images and compares them with transfer learning of established, pretrained deep neural networks, like the AlexNet, and the Visual Geometry Group (VGG) network, to the domain of brain asymmetry imaging.

The paper is laid out as follows. Section 2 presents related work that employed artificial neural networks for clinical diagnosis. Section 3 describes the computational framework for processing and classification of brain asymmetry images. Section 4 provides information on the MRI data sources used in the study. Section 5 describes the experiments and discusses the results. Section 6 includes a discussion of the topic, and Section 7 presents the conclusions.

2. Related Work

The CNN architecture has been used widely for processing and classifying images [13]. This section focuses on recent research efforts that are pertinent to this work.

Researchers in [14] focused on the diagnosis of MCI with a 2D CNN based on the LeNet-5 architecture. Functional MRI was used as an imaging source. The performance for the MCI data reached 73.4% of accuracy, 82.2% of precision, and 92.3% of recall.

Another work[15] combined various sources of clinical information and protocols of 1851 participants from the ADNI database. The authors proposed a diagnosis approach for dementia that uses a multilayer perceptron and a Convolutional Bidirectional Long Short-Term Memory and run Monte Carlo simulations[16]. The best available accuracy was 86%.

In [17] features extracted by Principal Component Analysis[18] were fed to a Regularized Extreme Learning Machine (RELM)[19] to classify input patterns into AD, MCI, and HC. The paper reported that the RELM improved classification accuracy compared to multiple kernel SVM and Import Vector Machine (IVM): binary classification of AD and MCI increased from 75.33% to 80.32%, whilst multiclass classification reached 76.61%. The latest 3D CNN perform well on medical imaging data. For instance, in [20], a 3D CNN architecture, which used 12 convolutional layers and a logistic regression layer at the output, was applied to a binary classification of patients with mild cognitive impairment (c-MCI) who had progressed to Alzheimer's Disease vs healthy cognitive patients (HC), and the classification of patients with a stable form of MCI (s-MCI) vs HC. The authors reported an accuracy of 87% and 76%, respectively.

In another work[21], the classification performance of a 3D VGG network in diagnosing AD was investigated. The researchers used the VGG16 model which consists of convolutional layers organized into four groups. The first and the second group contain two convolutional layers each. The third and the fourth group contain three layers each and a pooling layer follows them. T1-weighted MRIs of the ADNI and MRIs of the OASIS databases were used for classifiers' training and testing. Five-fold cross-validation was used and the classification accuracy reached 73.4% for ADNI data and 69.9% for the Open Access Series of Imaging Studies (OASIS) data.

The composition of functional MRI and Mini-Mental State Examination (MMSE) measures were also tested with 3D VGG network[22]. Feature selection procedure on MMSE was performed using linear least square regression (LLSR) tree regression, bagging-based ensemble regression and support vector regression. The algorithm recognized AD with a mean accuracy of 85.27%.

More complex models have been presented in the papers [23] [24]. A combination of deep learning models consisting of the fusion of two multilayer perceptrons (MLP) and CNN VGG-11 networks was investigated by Qiu et al. [23]. Prediction of MCI based on MRI and cognitive test score biomarkers was achieved with an accuracy of 90.9%. Another complex convolutional model was proposed by Spasov et al. [24]. The model consisted of AlexNet and Xception CNN architectures and used concatenated features from imaging and various non-imaging predictors. The obtained accuracy reached 86% by grouping imaging data and clinical test scores.

As one can notice, complex biomarkers are tested often with classification algorithms. In this way, [25] analyzed three groups of biomarkers, such as mental task performance scores, digital (Statistical) and imaging biomarkers (fNIRS), by applying CNN. The classification results received from each group of biomarkers demonstrated the advantage of the imaging biomarkers, which showed an accuracy of 90.62% in the detection of MCI.

Another study[26] used MRI imaging and non-imaging (age, ApoE4, TAU, cognitive test results) data for the prediction of AD. Regression analysis investigated the correlation between images and other clinical data, and deep learning based on convolutional autoencoders with Z-manifold block performed the classification task. AD was detected with an accuracy of 86% using all ranges of biomarkers.

CNNs have demonstrated promising results in distinguishing between different types of dementia and in [27] the investigators looked for the predictive power of CNN in differentiating between AD and dementia with Lewy bodies (DLB). They used brain scans obtained with perfusion single-photon emission computer tomography (SPECT). The reported accuracy was 93.1%, 89.3% and 92.4% for DLB vs healthy individuals, DLB vs AD and AD vs NL healthy individuals, respectively.

Another important direction in the study of Alzheimer's disease is that of risk estimation of its development from the early stages of cognitive decline, such as the conversion of MCI to AD examined in[28]. That work analyzed the structural hippocampal MRI using a deep learning framework for processing right and left hippocampal images in separate streams. The time-to-event prognosis of the progression of MCI to AD was conducted using LASSO regularized Cox regression model. The model generated an overall risk score for the disease progression: AD was detected with an accuracy of 90%, and the progression of MCI to AD with an accuracy of 76.2%. A combination of imaging and cognitive measures improved the performance by 10% for progressive MCI.

Research papers on the diagnosis of Mild Cognitive Impairments that employed CNN architectures are summarized in Table 1. The latest trends in AD and MCI diagnosis using ML are presented in[29].

Non-MRI methods in MCI and AD diagnosis are well described in the contemporary literature. Thus, the study[30] explored longitudinal changes in brain-electrical connectivity of patients with MCI and the conversion of this form of cognitive decline to Alzheimer's Disease. The research was based on Hierarchical clustering, which employed Electroencephalographic (EEG) signal and estimated dissimilarity between pairs of the recorded EEG signals by calculating the network density. Network density reduction was registered in patients with progressive to AD forms of MCI.

In another study[31], the authors used non-linear features and a probabilistic neural network for the prediction of MCI and AD. EEG signals were collected from frontal, parietal and occipital lobes of subjects with cognitive impairment and Alzheimer's Disease and processed with empirical wavelet transform, the so-called MUSIC-EWT. Non-linear indices of frequency bands were analyzed using one-way ANOVA, and the most discriminative ones were classified with an Enhanced Probabilistic Neural Network (EPNN).

Another diagnostic approach based on fuzzy logic classification algorithm was proposed in[32]. EEG data collected from AD, EMC and the healthy subjects were processed with Discrete Wavelet Transform and analyzed by computing the Dispersion Entropy Index from signal sub-bands. The most discriminative features were trained and tested with a fuzzy logic algorithm to distinguish between patients' classes. The method demonstrated an 82.6 – 86.9% accuracy for detecting AD and MCI.

Other than EEG, functional biomarkers, such as MEG, fMRI, and PET, can also be applied for the diagnosis of dementia and its stages [33, 34]. However, a detailed review of these methods is considered out-of-scope since the paper is focused on MRI.

Table 1. CNN-based methods in medical diagnosis of dementia

Reference	Pathology	Method	Performance
20	AD, sMCI, cMCI	3D CNN	Acc cMCI vs HC- 87%, Acc sMCI vs HC-76%, Acc AD vs HC-99%
15	Dementia	MLP + ConvBLSTM	Acc-86%
17	AD, MCI	Unsupervised DL RELM	Acc AD vs EMCI-80.32%, Acc multiclass-76.61%
21	AD	3D VGG	Accuracy: 73.4% - ADNI dataset, 69.9% - OASIS dataset
14	MCI	2D CNN based on LeNet-5	Acc 73.4%, Prec 82.2%, Recall 92.3%, F1 – 87%
23	MCI	2 MLP models + fusion of CNN VGG-11	Acc 90.9%
27	AD, DLB	CNN	Acc DLB vs NL-93.1%, Acc DLB vs AD-89.3%, Acc AD vs NL-92.4%
25	MCI	CNN	Acc- 90.62%,
26	AD	DL based on convolutional autoencoders	Acc 84%,
22	AD	3D CNN VGG	Acc-85.27%
28	AD, MCI	CNN	Acc AD vs NC – 90% Acc MCI vs AD 76.2%
24	Progressive MCI	AlexNet + Xception CNNs	Acc- 86%, sensitivity- 87.5%, specificity -84%

3. Computational Framework for Processing and Classification of Brain Asymmetry Images

In contrast to the work mentioned above that used MRI as a source of data, the proposed framework, illustrated in Fig. 1, is based on brain asymmetry images. The various stages of the data processing pipeline are presented in the following subsections.

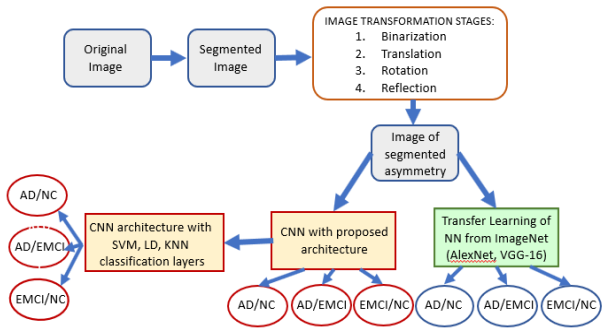

Fig. 1. Image transformations and generation process of brain asymmetry images for deep learning classification proposed.

3.1. *Image preprocessing stages*

The first preprocessing stage is image normalization, which brings the pixel intensity values of all imaging data to one standard. Each given grayscale image can be represented as a histogram of its gray levels. Gray values of a poorly contrasted image are clustered mainly in the center of the histogram. A histogram normalization method spreads the pixel values in a way that fills the entire available pixel's intensity range between 0 and 255. In our approach, MRI brain images are normalized using the histogram stretching technique.

The second stage is a routine procedure in image processing called image resizing, where all images are resized to one standard fixed size. The purpose of resizing is to fit the images into a certain dimensionality space. Very often, the size of big imaging data has to be reduced to speed up a machine learning process and minimize local storage requirements. In the current research, the images are resized to 256×256 pixels with three channels by replicating the grayscale image three

times to create three channels, extending the dataset that forms the input of the deep learning classification stage.

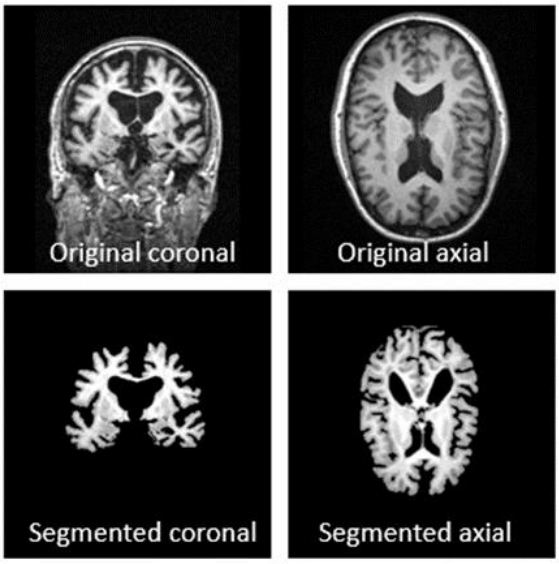

Fig. 2. MRI slices in coronal and axial planes in original form and after processing with segmentation algorithm.

3.2. *Brain segmentation methods including segmentation of hemispheric asymmetries*

In this stage, normalized and resized images are processed using brain segmentation algorithms (see Fig. 2), which aim to localize an object of interest or the image boundaries. The process concerns partitioning an image into sets of pixels, or segments, united under a special set of rules. In the case of MRI, segmentation can be performed on 2D images separated from an image sequence or on 3D series. If 2D images are segmented slice-by-slice, they can be used to construct a 3D model. Nevertheless, despite the advantages of 3D, most clinical imaging procedures these days are still 2D. Moreover, the training of 3D volumetric images with 3D CNN slows down their processing without significant improvement in the performance of the classifier as reported in [35]. A favourable feature of image asymmetries is that they can be obtained from frontal and horizontal MRI slices only- a sagittal plane is not relevant for asymmetry. This can facilitate practical implementations of the asymmetry biomarker and CNNs in routine healthcare checks using 2D image slices and off-the-shelf affordable hardware.

Typically, a scanned image incorporates the skull and a nonbrain area as well as white matter (WM) brain tissue, gray matter (GM) brain tissue, and cerebrospinal fluid (CSF). Therefore, a common approach in MRI processing involves the extraction of nonbrain tissues before the brain segmentation methods can be used.

Although there is no single method appropriate for all images because of image diversity, presence of noise and artefacts, a segmentation method that has been developed for one imaging context can be adapted to another class of images.

The segmentation method that is used in the research belongs to the group of intensity-based methods, which includes thresholding and region-growing or region-based types[38,39,40]. The three main MRI brain tissue types are WM, GM and CSF, which can be easily distinguished due to their differences in pixel intensity levels. However, the presence of noise, artefacts, overlapped objects, and inhomogeneity of the tissues is an objective factor that can require the incorporation of additional tools and the implementation of advanced techniques. Biases during the brain segmentation can be corrected by adjusting the level of thresholding via changing the values of the upper and lower boundaries; an approach adopted in this work. Fig. 2 demonstrates the performance of the segmentation algorithm on an MRI slice.

The next level of segmentation helps to detect differences between the right and left hemispheres defining a brain asymmetry image. It is important to note that we use our own segmentation algorithms to understand asymmetries' nature and control the feature collection process. The adopted technique and the robustness of the generated brain asymmetry images and features for class separation were verified in [6], and a Matlab implementation is available online at: https://www.mathworks.com/matlabcentral/fileexchange/85628-asymmetry-detection-of-the-mri-brain.

The method is based on the finding that there is a loss of gray and white matter at the initial stage and along with the development of the neurodegenerative disorder, which leads to variations in the symmetry of the brain's structure. Initially the symmetry between the left and right hemispheres of the brain increases. However, the progression of the disease increases the degree of asymmetry as the left-sided hemispheric lateralization of a healthy individual gradually becomes right-sided with the development of severe dementia such as Alzheimer's Disease (see Refs. 4 and 5). For a cognitively normal person, Fig. 3 demonstrates the variations in the anatomy of the left and right hemispheres.

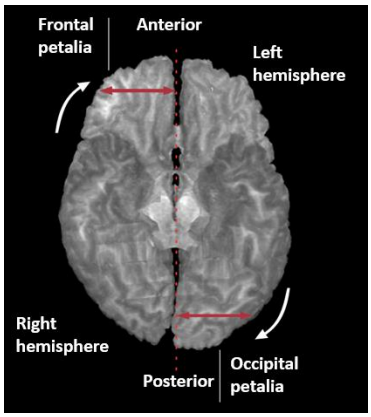

Fig. 3. Lateralisation of a healthy brain. (Source: CDI, Oswaldo Cruz German Hospital - Fleury Group / São Paulo 2015.)

Differences in the symmetry of the two hemispheres can be detected through segmentation. The process of image analysis and asymmetry detection was discussed analytically in[6] and is briefly presented next for completeness: (i) it involves detecting the vertical line of brain symmetry. This is assigned for mirroring the left hemisphere to the right and repeating the same process in the opposite direction; (ii) the original image is subtracted from its reflected version. Asymmetrical regions of the brain, whose pixels have different intensity levels according to the level of asymmetry, are segmented from the image by means of image matrix operations. An example of the visual changes of an image

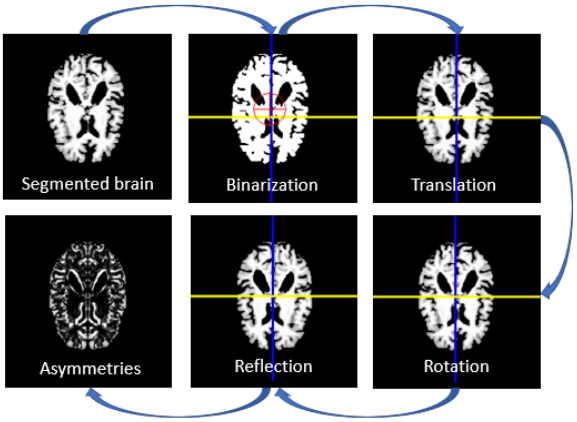

Fig. 4. Image transformation stages from the segmented brain to the detection of brain asymmetries.

following the above-mentioned processing stages is shown in Fig. 4.

3.3. *Architectural configurations of the CNN and transfer learning*

This stage of the framework focuses on the identification of early and progressive dementia considering brain asymmetries as a potential biomarker. The problem is formulated as a set of binary classification tasks.

Deep learning is not always the best approach to medical diagnosis because of the "black box" issue. We applied the latest DL methods to investigate their potential use in the identification of early mild cognitive impairment using MRI of brain asymmetries. The indicated asymmetries, which are represented by differences in pixel values between the left and right lobes, can potentially enhance the level of interpretability of the features generated under the convolutional transformations. The previous work[7], which focused on transfer learning for asymmetry images, showed that pretrained AlexNets, which belong to the class of CNNs, are suitable for MRI processing. Moreover, it identified benefits when extra Softmax or SVM layers are added to the base model. During transfer learning, the networks, which were pretrained on ImageNet, use their learned parameters as initialization for the new training of the whole architecture with asymmetry images- a process commonly called fine-tuning. Fine-tuning is based on the stochastic gradient descent with momentum, as described in Section 5.

Building on this work, deep learning architectures with CNNs remain at the core of our approach but are enriched with one more transfer learning architecture, the so-called VGG16 model that is deeper than AlexNet, as well as new CNN-based models that are designed and trained on MRI data from the start. The new models share a common CNN module as a base network and are equipped with separate Softmax, SVM, LD or KNN classification modules. The choice of these methods was based on previous work that provided evidence that they perform well on their own when used for the classification of brain asymmetries[6].

In the base CNN architecture (see Fig.5), the first five convolutional layers play the role of feature detectors and there is one fully connected layer. Additional layers consist of Local Response Normalization (LRN), Batch Normalization (BN), average pooling, dropout and Softmax layers. Overall, there are 258,064 neurons and 12.8 million learnable parameters. The LRN uses non-linear functions, known as Rectified Nonlinearity Units (ReLUs), which speed up training by normalizing the

feature maps and removing the negative value. The Batch Normalization layer makes the deep learning process faster and more stable by the standardization of the layers' inputs. Recentring and rescaling operations are at the base of this process. Average pooling layers perform dimensionality reduction of the images implementing a downsampled operation on the input layers. Dropout clamps to zero the output signals of hidden neurons whose probability of activation is 0.5 or lower to reduce overfitting. The first convolutional layer requires an input image of size 256×256×3, i.e. 256 pixels wide, 256 pixels high, and three color channels, which are artificially created by replicating a grayscale image of brain asymmetry three times to create three channels in order to augment the dataset and facilitate integration with the core CNN architecture and the pretrained CNNs, as explained below. This layer includes 16 convolutions of size 5×5×3 and uses stride = 1 (the stride indicates the step size with which the filter/convolution moves over the image matrix). The second layer has 32 convolutions of size 3×3×3 with stride = 2, while the third layer is a copy of the second layer but stride =1. The fourth and fifth layers have 64 convolutions of similar sizes of 3×3×3 with stride = 2. Each convolution layer is followed by Batch Normalization and ReLU layers. Average pooling layers follow the third and the fifth layers' convolutions. A fully connected layer puts together all feature outputs from previous layers and sends them to the activation unit (e.g. Softmax). Fig. 5 illustrates the core CNN architecture. In this instantiation (additional instantiations are discussed in Section 5), the Softmax layer normalizes the outputs that are used as classification probabilities by the output layer for the binary diagnostic task.

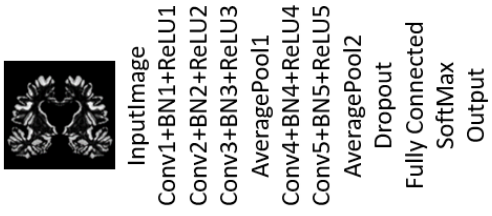

Fig. 5. An instantiation of the core CNN architecture that is equipped with a standard Softmax module.

In comparison, pretrained CNNs like AlexNet and VGG16 were originally configured and trained for 1000 classes using ImageNet data. The AlexNet architecture consists of 8 layers, has a size of 227MB and includes 61 million parameters. The input dimensionality is 227×227×3 (images should be 227 wide, 227 high, 3 color channels). The VGG16 architecture is much bigger than the trained model c. 515MB. This network has 16 layers and 138 million parameters, and the input dimensionality is 224×224×3. Both architectures require three channels (number 3 in input dimensionality) as they were originally designed to process ImageNet RGB images. As mentioned above in the case of the base CNN architecture, this requirement is addressed by replicating the grayscale image three times to create the three channels.

4. MRI Data Repository

The MRI data were obtained from the Alzheimer's Disease Neuroimaging Initiative (ADNI) database (adni.loni.usc.edu). The ADNI was introduced as a public-private partnership led by Dr M.W. Weiner in 2003. Details about the project and up-to-date information are available at www.adni-info.org.

The used dataset includes 600, 2D images which are equally divided between three classes of AD, EMCI and NC subjects. T1-waited MRI data from the ADNI3 database were obtained from 50 patients with Mild Cognitive Impairment (EMCI) at the age between 55 and 65 years old, 50 patients with Normal Cognition (NC) at the age between 55 and 65 years old, and 50 patients with Alzheimer's Disease (AD) at the age between 65 and 90 years old. The age range between 55 and 65 years for the EMCI and NC groups was chosen to eliminate the ageing effect on the MRI data. Images were taken from the same type of 3T scanners, Siemens Medical Solutions (http://adni.loni.usc.edu/methods/mri-tool/mri acquisition). Thus, 600 image dataset of 150 subjects was obtained by extracting four central slices from each MRI brain. The chosen slices represented the most affected brain areas (according to the literature, frontal and parietal zones as well as hippocampus and amygdala). Examples of the created asymmetry images are exhibited in Fig. 6.

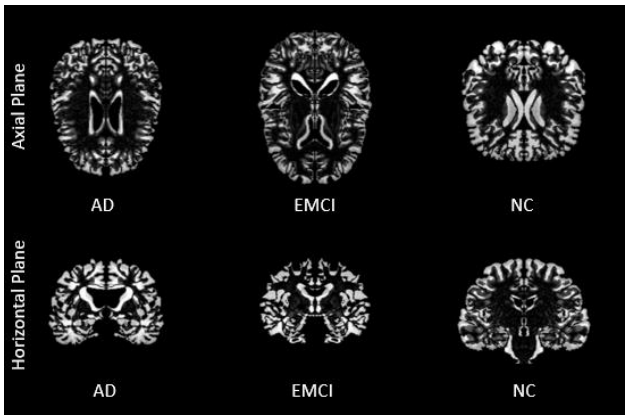

Fig. 6. Sample of input images of segmented asymmetries for AD, EMCI and NC classes

5. Experimental Study

The vast majority of algorithms work by training deep networks on high-performance computing infrastructures (e.g. cloud, GPU clusters). We explore an alternative approach that exploits the characteristics of asymmetry images and uses commodity hardware, i.e. the hardware is off-the-shelf, affordable and easy to obtain; it is functional and suitable for processing asymmetry images with deep networks. The experiments presented in this section were conducted using the following hardware: PC running Windows10 Enterprise, CPU Intel i7-7700 at 3.60 GHz, 16 GB RAM. The computational framework has been developed using Matlab.

In the first experiment, CNNs from the ImageNet (AlexNet, VGG16) are retrained using transfer learning, and their classification performance is compared with the newly established classifier (Section 3.3), which consists of the CNN core plus Softmax module.

The second experiment compares different instances of the CNN core module equipped with a Softmax, SVM, LD or KNN module. This module is connected to the fully connected layer to produce the output.

As mentioned above, the dataset includes 600 images of segmented asymmetries from 150 patients (samples are shown in Fig. 6). Four brain slices from the most affected areas were taken from each patient. Segmented asymmetry images had a size of 256×256×3, where to create three channels, as mentioned in Section 3.3, the 600 grayscale images were replicated three times to create the three channels.

The experiments were run with balanced datasets, i.e. the number of patients and their corresponding MRI images were equally distributed between the three classes. Each binary classification task, namely EMCI vs NC, AD vs NC, and AD vs EMCI, used 400 images, and several independent runs with each deep learning architecture were performed, as described in the following sections, i.e. each model's architecture was fixed but it was trained from random initial weight conditions at each run.

The number of training epochs, *n*, was set to 11, the mini-batch size was 128 and the frequency of checking the validation metric was equal to 50. Lastly, a small initial learning rate equal to 0.0001 was adopted, whilst training followed the stochastic gradient descent with momentum (SGDM) method (see Ref 35). These settings were based on preliminary experiments reported in[7]. Those and additional experiments included tests with the different batch sizes of 32, 64 and 128 and a variable number of training epochs from 5 to 30. The experimental CNN architectures were based on 3, 5, 7, and 9 CNN layers.

Training, validation and testing data described in this paper are selected randomly on a patient level, and no images from validation or test patients are included in the training set. In addition, the data is shuffled with each training epoch. A similar classification approach for medical diagnosis is used in the relevant literature; see Refs. 36, 37. The data were split into 80% for training, 10% for validation and 10% for testing. The same training, validation and testing datasets were used in all experiments with CNN models, including the transfer learning architectures.

An example of learning curves for the training accuracy and loss/error of a 5CLNN-Softmax is provided in Fig.7.

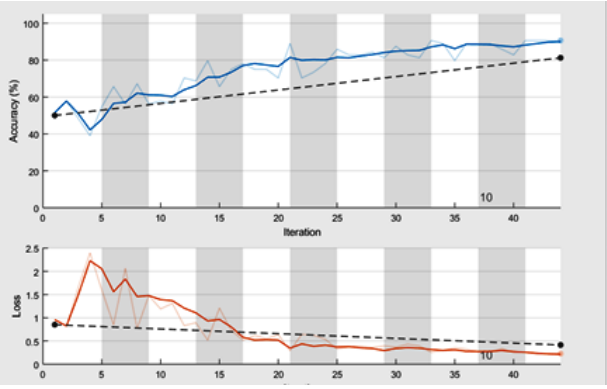

Fig.7. Example of training accuracy and error over 11 epochs for a 5CLNN-Softmax. The horizontal axis indicates

iterations/weight updates. Top graph: smoothed (moving average) training accuracy (thick blue line) and training accuracy on each mini-batch (thin blue line). Bottom graph: smoothed training loss (thick red line) and training loss on each mini-batch (thin red line).

5.1. *Experiment 1*

In this experiment, the two pretrained neural networks, AlexNet and VGG-16, are fine-tuned by substituting the last three layers of the original architecture with a fully connected layer, Softmax and output layers which are adjusted to the number of classes in the task. The layer replacement is the first step of fine-tuning and it is followed by the training of the whole network.

Table 2 provides comparative performance in testing based on ten independent runs from random initial conditions for each architecture. In this table, the newly established classifier, CNN core plus SoftMax, is denoted by 5CLNN.

Performance measures such as Accuracy, F1-score and AUC demonstrate the overall improvement in the identification of dementia using 5CLNN. The average accuracy across all diagnostic tasks for 5CLNN is higher than the accuracy of AlexNet by 1.3% and that of VGG-16 by 5.39%. F1-score demonstrates similar differences in performance with 5CLNN better by 1.4% compared to AlexNet, and by 5.5% compared to VGG-16. The 5CLNN achieves the highest AUC in the identification of AD vs NC. Early changes in the brain are diagnosed with an accuracy of 86.4%, precision of 83%, recall of 89.1% and an F1-score of 86.0%. The diagnostic performance in AD vs EMCI is 79.8% in terms of accuracy, 81% in precision, 79.1% in recall, and 80.1% in the F1-score using 5CLNN.

The performance of AlexNet and 5CLNN was tested further to investigate how consistent the differences were. Thirty additional independent runs were conducted for each subset of 400 asymmetry images (see Table 3).

Table 2. Average performance in testing based on 10 independent runs for AlexNet, VGG16, 5CLNN classifiers for three binary datasets: AD vs EMCI, EMCI vs NC, and AD vs NC.

Classifiers with datasets	Accuracy	Precision	Recall	F1-score	AUC
AlexNet					
AD vs EMCI	0.787 ± 0.021	0.790 ± 0.020	0.785 ± 0.023	0.787 ± 0.021	0.875 ± 0.006
EMCI vs NC	0.858 ± 0.015	0.850 ± 0.016	0.863 ± 0.013	0.856 ± 0.015	0.893 ± 0.002
AD vs NC	0.882 ± 0.025	0.863 ± 0.026	0.896 ± 0.024	0.800 ± 0.025	0.938 ± 0.001
VGG-16					
AD vs EMCI	0.708 ± 0.026	0.720 ± 0.023	0.702 ± 0.021	0.711 ± 0.022	0.826 ± 0.003
EMCI vs NC	0.823 ± 0.020	0.790 ± 0.024	0.845 ± 0.019	0.816 ± 0.021	0.902 ± 0.001
AD vs NC	0.873 ± 0.030	0.870 ± 0.030	0.874 ± 0.032	0.872 ± 0.031	0.921 ± 0.005
5CLNN					
AD vs EMCI	0.798 ± 0.023	0.810 ± 0.021	0.791 ± 0.025	0.801 ± 0.023	0.874 ± 0.003
EMCI vs NC	0.864 ± 0.031	0.830 ± 0.032	0.891 ± 0.026	0.860 ± 0.028	0.928 ± 0.002
AD vs NC	0.901 ± 0.030	0.950 ± 0.026	0.866 ± 0.031	0.906 ± 0.028	0.941 ± 0.004

Table 3. Average performance in testing based on 30 additional independent runs for AlexNet and 5CLNN classifiers using the same binary datasets.

Classifiers with datasets	Accuracy	Precision	Recall	F1-score	AUC
AlexNet					
AD vs EMCI	0.771 ± 0.022	0.760 ± 0.020	0.777 ± 0.024	0.769 ± 0.022	0.880 ± 0.006
EMCI vs NC	0.860 ± 0.015	0.870 ± 0.016	0.853 ± 0.016	0.861 ± 0.016	0.898 ± 0.002
AD vs NC	0.882 ± 0.026	0.860 ± 0.027	0.901 ± 0.024	0.880 ± 0.026	0.952 ± 0.002
5CLNN					
AD vs EMCI	0.803 ± 0.023	0.810 ± 0.021	0.799 ± 0.025	0.804 ± 0.024	0.870 ± 0.003
EMCI vs NC	0.878 ± 0.031	0.850 ± 0.033	0.900 ± 0.027	0.874 ± 0.030	0.931 ± 0.002
AD vs NC	0.911 ± 0.032	0.930 ± 0.028	0.895 ± 0.032	0.912 ±0.030	0.948 ± 0.004

The obtained results appear in line with the previous ones (cf with Tables 2 and 3). In terms of accuracy and F1-score, the 5CLNN outperforms the AlexNet by 3.20% and 1.62% for AD vs EMCI, by 1.75% and 1.90% for EMCI vs NC and by 2.80% and 1.68% for AD vs NC sets.

The statistical significance of these differences was evaluated using Wilcoxon-Mann-Whitney ranksum test[33]. This pairwise non-parametric test was applied to prove that the accuracy of 5CLNN is better than the accuracy of AlexNet architecture for AD vs EMCI, EMCI vs NC and AD vs NC datasets (see Table 4). The null hypothesis is based on the statement that we cannot easily create a new architecture that will perform at the same level or even outperform the CNN model AlexNet. If the null hypothesis is rejected, this opens the opportunity for new configurations with at least the same performance and potential improvement.

Table 4. Statistical significance of testing based on 30 independent runs for AlexNet and 5CLNN.

Classifiers	AD vs EMCI	EMCI vs NC	AD vs NC
p	0.01	0.01	0.01
h	1	1	1

The test returns a *p*-value equal to 0.01 for each imaging subset and shows a logical value of the test decision $h = 1$, which indicates a rejection of the null hypothesis at the 5% level of significance. Thus, the outperformance of 5CLNN is proven by these measures. Also, it is worth reporting that the average time spent for training, validation and testing was 29 min for 5CLNN, 36 min for AlexNet and 546 min for VGG-16 using the same hardware in all cases.

5.2. *Experiment 2*

Table 5. Average performance out of 10 runs for the 5CLNN with different classification modules (Softmax, SVM, LD and KNN) in the three binary datasets.

Classifiers with datasets	Accuracy	Precision	Recall	F1-score	AUC
5CLNN-Softmax					
AD vs EMCI	0.798 ± 0.023	0.810 ± 0.021	0.791 ± 0.025	0.801 ± 0.023	0.874 ± 0.003
EMCI vs NC	0.864 ± 0.031	0.830 ± 0.032	0.891 ± 0.026	0.860 ± 0.028	0.928 ± 0.002
AD vs NC	0.901 ± 0.030	0.950 ± 0.026	0.866 ± 0.031	0.906 ± 0.028	0.941 ± 0.004
5CLNN-SVM					
AD vs EMCI	0.789 ± 0.025	0.815 ± 0.020	0.774 ± 0.028	0.794 ± 0.024	0.873 ± 0.003
EMCI vs NC	0.867 ± 0.020	0.750 ± 0.023	0.880 ± 0.018	0.865 ± 0.020	0.900 ± 0.001
AD vs NC	0.879 ± 0.040	0.869 ± 0.041	0.888 ± 0.037	0.878 ± 0.039	0.940 ± 0.001
5CLNN-LD					
AD vs EMCI	0.804 ± 0.020	0.829 ± 0.018	0.790 ± 0.023	0.809 ± 0.020	0.909 ± 0.002
EMCI vs NC	0.873 ± 0.012	0.850 ± 0.019	0.891 ± 0.011	0.870 ± 0.016	0.968 ± 0.002
AD vs NC	0.886 ± 0.035	0.891 ± 0.032	0.881 ± 0.037	0.886 ± 0.035	0.920 ± 0.002
5CLNN-KNN					
AD vs EMCI	0.723 ± 0.017	0.740 ± 0.014	0.716 ± 0.020	0.728 ± 0.017	0.893 ± 0.003
EMCI vs NC	0.833 ± 0.032	0.800 ± 0.036	0.856 ± 0.030	0.827 ± 0.033	0.905 ± 0.002
AD vs NC	0.874 ± 0.036	0.855 ± 0.038	0.889 ± 0.031	0.872 ± 0.035	0.903 ± 0.003

The second experiment focuses on the comparison of the classification performance of different instances of the core 5CLNN. To this end, in Experiment 2, Support Vector Machine (SVM), Linear Discriminant (LD), and K-Nearest Neighbor (KNN) classification modules replace the Softmax layer, which was used in Experiment 1. The SVM module uses a linear kernel function with a box constraint level equal to 1. The KNN module uses Euclidian distance with number of neighbors equal to 1. The four instantiations of the model are shown in Fig.8.

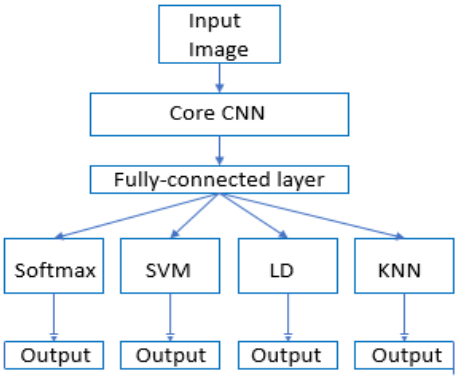

Fig. 8 Combining the 5CLNN core with alternative classification modules: Softmax layer (original configuration), SVM module, LD module and KNN module.

Table 5 shows the average performance (out of 10 runs) for each model - 5CLNN-SoftMax, 5CLNN-SVM, 5CLNN-LD and 5CLNN-KNN- in the three classification tasks.

The 5CLNN-LD architecture achieves the best average performance over all binary problems. Its accuracy is higher than the 5CLNN with Softmax by 0.63% for AD vs EMCI and 0.87% for EMCI vs NC. However, 5CLNN-LD architecture shows lower performance than 5CLNN-Softmax in the AD vs NC task. The 5CLNN-KNN architecture demonstrates lower performance than other models in all diagnostic tasks.

A Wilcoxon ranksum test, as before, was used to check if the performance differences of the 5CLNN-LD model, although small, are significant compared to the second-best model, 5CLNN-Softmax. The null hypothesis (h) is that the differences in the performance of 5CLNN-LD and 5CLNN-Softmax are not significant. If the null hypothesis is rejected (h=1), one says that the differences are significant at the 5% level. The outcome of the Wilcoxon test is presented in Table 6.

Table 6. Statistical significance of the results based on 10 runs for the 5CLNN with Softmax and LD modules.

Classifiers	AD vs EMCI	EMCI vs NC	AD vs NC
p	0.0145	0.0145	0.0145
h	1	1	1
z	2.4442	2.4442	2.4442

The p-value of 0.0145, h equal to 1 and z-score of 2.4442 confirm the statistical significance of the obtained results.

6. Discussion

Although a variety of dementia prediction models, based on CNN and transfer learning, can be found in previous literature, the approach presented in this paper is tailored to MRI brain asymmetries, as a new potential biomarker in predicting cognitive decline and dementia. In this context, it investigates the potential of integrating the CNN feature detector modules with different classification modules, going beyond the standard CNN architectures with Softmax classification layers used in previous attempts

The experiments were conducted through the analysis of MRI brain asymmetries by CNN configurations that were trained to solve a set of binary classification problems. Various CNNs created from scratch or pretrained were evaluated, providing evidence of the diagnostic potential of these models when images of brain asymmetries are used. Pretrained CNNs were adapted to the new domain via transfer learning strategy and fine-tuned. The proposed 5CLNN core architecture was combined with SVM, LD and KNN modules and trained successfully and tested on images of brain asymmetries that were not used before.

The study's findings offer additional insight into the diagnosis of dementia, especially considering the detection of early mild cognitive impairment using the images of segmented asymmetry as a potential biomarker. Early changes in the brain (EMCI vs NC) were diagnosed by the proposed 5CLNN with an accuracy of 87.8%±3.1% over 30 training/testing runs. The model's ability to distinguish between AD and EMCI is 80.3%±2.3%, whilst the AD prediction score compared to NC samples is 91.1%±3.2%.

Also, the diagnostic accuracy of the two transfer learning models implemented, AlexNet and VGG16, in the early stages of cognitive decline (EMCI vs. NC) reached 86.0% ± 1.5% and 82.3% ± 2.0%, respectively. However, the proposed 5CLNN performed better than the transfer learning models in the tests conducted. The average accuracy across all diagnostic tasks for 5CLNN is higher than the accuracy of AlexNet by 1.8% and VGG-16 by 4.1%. Moreover, the training, validation, and testing time of the 5CLNN model is visibly shorter by 7 min (1.24 times) compared to AlexNet and by 517 min

(18.83 times) compared to VGG-16 using commodity hardware.

Another substantial finding of the study is that the model's performance using asymmetry images can be improved further by using an appropriate classification module. For instance, the best results for the 5CLNN were obtained when the model was equipped with an LD classification module. This scheme demonstrated, on average, 87.3±1.2% of accuracy for the identification of EMCI. In contrast, equipping the CNN core with a Softmax layer (typically used in CNN applications), an SVM module or a KNN module, generated average accuracy of 86.4%±3.1%, 86.7±2%, and 83.3±3.2%, accordingly.

The detection performance of created models based on images of segmented brain asymmetries is comparable to the results of the state-of-the-art literature (see Table 2) that used whole MRIs as a source of imaging data. The proposed CNN model demonstrates the accuracy of 87.8% in the diagnosis of early mild cognitive decline which is higher than that obtained with 3D CNN (87% for converted MCI and 76% for stable MCI)[20]. The proposed CNN (87.8%) overperformed LeNet-5 whose diagnostic prediction was 73.4% (see Ref.14), and combined AlexNet and Xception CNNs with the prediction of 86% in the diagnosis of progressive MCI[24]. Another study[25] used CNN trained via t-maps and reported the best accuracy of 90.62% in the detection of MCI, but no average performance results were provided. Also, the complex model[23] (MLP models + fusion of CNN VGG-11) predicts the MCI with an accuracy of 90.9%. In the diagnosis of AD, our model gives 91.1% of accuracy on average which is higher than in works[21,22,26,28] where it is equal to 73.4%, 85.27%, 84%, and 90%. At the same time, the performance of our model is lower than in[27] by 1.3%. However, the results (see Ref.27) are not based on the ADNI dataset but on proprietary data, the set of images is shorter than the one used in this work, and only the performance of the best CNN model that was trained is reported.

Despite the visible similarity in classification performance with other research methods, the models that were trained using segmented asymmetry images have notable advantages. It is important to note that we did not use fusion strategies, like joint models (see Ref. 22, 27), multiple combined biomarkers (see Ref.23-26), or 3D CNNs that process an enormous amount of data (see Ref. 20), increasing model complexity and imposing implementation requirements. The tendency of overfitting with segmented brain asymmetry images, which are focused on the affected areas, appears low with the use of dropout, and the model uses less features, which may shorten the training time.

Deployment of the framework into medical practice would of course require extensive experimentation with a larger number of patients than the 150 used in this study. Also, issues of bias could be avoided by performing experiments with asymmetry images generated from other MRI databases (e.g. OASIS) and segmentation of hemispheric asymmetries with SPM/VBM standard image preprocessing software.

7. Conclusions

The growth of medical information has shown the necessity of using new diagnostic methods based on computerized algorithms. Deep neural networks open new possibilities in processing and analyzing imaging and non-imaging medical data. Among other areas, these methods demonstrate potential in diagnosing neurodegenerative diseases at an early stage, which can benefit health care and social services.

A computerized diagnostic of MCI based on MRI data can be more accurate and informative than the cognitive psychological tests routinely used by medical practitioners. Automating the process lessens the work of radiologists, psychiatrists, gerontologists, and family doctors by providing a machine-supported diagnosis. In addition, detecting a mental decline in patients enables health services to provide early treatment that can help patients stay independent longer.

Early and precise diagnosis of medical pathology is crucial in many situations when timely and focused therapy can find the appropriate treatment and reduce risks for patients. To this end, the paper presented and validated a computational framework for the diagnosis of early and progressive dementia based on image analysis of brain asymmetries and deep learning architectures.

The proposed approach is effective in the detection of Mild Cognitive Impairment that can lead to the development of Alzheimer's Disease in 10-15% of cases, according to the literature. The framework was implemented and tested using commodity hardware exploiting the properties of asymmetry in MRI images when combined with transfer learning or neural networks trained from scratch with images of brain asymmetry. All schemes demonstrate consistent and robust performance

and indicate that the images of brain asymmetries can be used as an additional biomarker in the diagnosis of dementia.

The suggested computational framework can be potentially useful to other researchers working on the diagnosis of brain-related disorders or the processing and classification of other medical imaging data, especially in cases with unclear border and texture or low-scale structural changes, which are not visible to the human eye.

Future research includes many additional directions. The first of them is a longitudinal study of patients with cognitive decline. Observation of the structural and functional changes in brain asymmetry can add some more clarification to the development of the destructive process in the brain tissues.

Another line of research is an investigation of the white matter asymmetries. It remains unclear what pattern of asymmetries have AD, EMCI and NC individuals and how these patterns different from the asymmetries found in gray matter.

An important addition to the contemporary knowledge of the development of dementia is further studies of regional asymmetries. A more detailed investigation of regional asymmetries using supervised learning and transfer learning methods can potentially enhance our understanding of Alzheimer's Disease and dementia.

Acknowledgements

Data collection for this work was funded by the Alzheimer's Disease Neuroimaging Initiative (ADNI) (National Institutes of Health Grant U01 AG024904) and DOD ADNI (Department of Defense award number W81XWH-12-2-0012). The research presented in this paper was partially funded by a BEI School Award of Birkbeck College, University of London. For the purposes of open access, the author has applied a CC BY public copyright license to any author accepted manuscript version arising from this submission.

References

1. Z. Zhang, Y. Xie, F. Xing, M. McGough and L. Yang, Mdnet: A semantically and visually interpretable medical image diagnosis network. In: *Proceedings of the IEEE conference on computer vision and pattern recognition*, (IEEE, Honolulu, Hawaii, USA, 2017), pp. 6428-6436.
2. A. Segato, A. Marzullo, F. Calimeri, E. De Momi, Artificial intelligence for brain diseases: A systematic review, *APL bioengineering*. 4(4) (2020) p.041503.
3. M. Janelidze and N. Botchorishvili, Mild Cognitive Impairment. *Alzheimer's Disease: The 21st Century Challenge*, *91*, (IntechOpen, London, 2018).
4. C. Yang, S. Zhong, X. Zhou, L. Wei, L. Wang, S. Nie, The abnormality of topo-logical asymmetry between hemispheric brain white matter networks in Alzheimer's disease and mild cognitive impairment. *Frontiers in aging neuroscience*, 9 (2017), p.261.
5. H. Liu, L. Zhang, Q. Xi, X. Zhao, F. Wang, X. Wang, W. Men, Q. Lin, Changes in brain lateralization in patients with mild cognitive impairment and Alzheimer's disease: A resting-state functional magnetic resonance study from Alzheimer's disease neuroimaging initiative. *Frontiers in neurology*, 9 (2018), p.3
6. N.J. Herzog, G.D. Magoulas, Brain Asymmetry Detection and Machine Learning Classification for Diagnosis of Early Dementia, *Sensors*. 21(3) (2021) p.778
7. N.J. Herzog, and G.D. Magoulas, Deep Learning of Brain Asymmetry Images and Transfer Learning for Early Diagnosis of Dementia. In *International Conference on Engineering Applications of Neural Networks* (Springer, Cham, June 2021), pp. 57-70.
8. A.S. Lundervold, A. Lundervold, An overview of deep learning in medical imaging focusing on MRI, *Zeitschrift für Medizinische Physik*, 29(2) (2019) pp.102-127.
9. N. Yamanakkanavar, J. Y. Choi, B. Lee, MRI segmentation and classification of human brain using deep learning for diagnosis of Alzheimer's disease: a survey, *Sensors*. 20(11) (2020) p.3243.
10. M. Z. Alom, T. M. Taha, C. Yakopcic, S. Westberg, P. Sidike, M. S. Nasrin, B. C. Van Esesn, A. A. S. Awwal and V. K. Asari: The history began from alexnet: A comprehensive survey on deep learning approaches. arXiv:1803.01164 (2018).
11. Y. Tang, Deep learning using linear support vector machines. arXiv:1306.0239 (2013).
12. N. Tajbakhsh, J. Y. Shin, S. R. Gurudu, R. T. Hurst, C. B. Kendall, M. B. Gotway and J. Liang, Convolutional neural networks for medical image analysis: Full training or fine tuning? *IEEE transactions on medical imaging*, 35(5) (2016), pp.1299-1312.
13. R. Yamashita, M. Nishio, R.K.G. Do and K. Togashi, Convolutional neural networks: an overview and application in radiology. *Insights into imaging*, 9(4) (2018), pp.611-629.
14. L Heising and S. Angelopoulos, January. Early Diagnosis of Mild Cognitive Impairment with 2-Dimensional Convolutional Neural Network Classification of Magnetic Resonance Images. In *Proceedings of the 54th Hawaii International Conference on System Sciences*, Hawaii, United States, 5–8 January 2021, p. 3407.
15. D. Stamate, R. Smith, R. Tsygancov, R. Vorobev, J. Langham, D. Stahl and D. Reeves, Applying Deep Learning to Predicting Dementia and Mild Cognitive

Impairment. In: I*FIP International Conference on Artificial Intelligence Applications and Innovations*, pp. 308-319. (Springer, Cham, 2020).
16. A. M. Johansen, L. Evers and N. Whiteley, Monte Carlo methods. Lect. Notes, University of Bristol, 2010. Available online at https://warwick.ac.uk/fac/sci/statistics/staff/academic-research/johansen/teaching/mcm-2007.pdf .
17. R. K. Lama, J. Gwak, J. S. Park and S.W. Lee, Diagnosis of Alzheimer's disease based on structural MRI images using a regularized extreme learning machine and PCA features. *Journal of healthcare engineering*, 1 (2017), 1-11.
18. H. Abdi and L. J. Williams, Principal component analysis. *Wiley Interdisciplinary Reviews: Computational Statistics*, 2(4), (2010), pp.433-459.
19. S. Ding, X. Xu and R. Nie, Extreme learning machine and its applications. *Neural Computing and Applications*, 25(3) (2014), pp.549-556.
20. S. Basaia, F. Agosta, L. Wagner, E. Canu, G. Magnani, R. Santangelo and M. Filippi, Alzheimer's Disease Neuroimaging Initiative.: Automated classification of Alzheimer's disease and mild cognitive impairment using a single MRI and deep neural networks. *NeuroImage: Clinical*, 21, (2019) p.101645.
21. E. Yagis, L. Citi, S. Diciotti, C. Marzi, S. W. Atnafu and A. G. S. De Herrera, 2020, July. 3D Convolutional Neural Networks for Diagnosis of Alzheimer's Disease via Structural MRI. In *IEEE 33rd International Symposium on Computer-Based Medical Systems (CBMS)* (IEEE, Rochester, MN, USA, 2020),pp. 65-70.
22. N. T. Duc, S. Ryu, M. N. I. Qureshi, M. Choi, K. H. Lee and B. Lee. 3D-deep learning based automatic diagnosis of Alzheimer's disease with joint MMSE prediction using resting-state fMRI. *Neuroinformatics*. 18(1) (2020), pp.71-86.
23. S. Qiu, G. H. Chang, M. Panagia, D. M. Gopal, R. Au and V. B. Kolachalama. Fusion of deep learning models of MRI scans, Mini–Mental State Examination, and logical memory test enhances diagnosis of mild cognitive impairment. *Alzheimer's & Dementia: Diagnosis, Assessment & Disease Monitoring*, 10 (2018), pp.737-749.
24. S. Spasov, L. Passamonti, A. Duggento, P. Lio, N. Toschi and Alzheimer's Disease Neuroimaging Initiative. A parameter-efficient deep learning approach to predict conversion from mild cognitive impairment to Alzheimer's disease. *Neuroimage*. 189 (2019), pp.276-287.
25. D. Yang, K. S. Hong, S. H. Yoo and C. S. Kim, Evaluation of neural degeneration biomarkers in the prefrontal cortex for early identification of patients with mild cognitive impairment: an fNIRS study. *Frontiers in Human Neuroscience*. 13 (2019), p.317.
26. F. J. Martinez-Murcia, J. M. Górriz, J. Ramírez and A. Ortiz. Convolutional neural networks for neuroimaging in Parkinson's disease: is preprocessing needed? *International Journal of Neural Systems*. 28(10) (2018), p.1850035.
27. T. Iizuka, M. Fukasawa and M. Kameyama. Deep-learning-based imaging-classification identified cingulate island sign in dementia with Lewy bodies. *Scientific reports*. 9(1) (2019), pp.1-9.
28. H. Li, M. Habes, D. A. Wolk, Y. Fan and Alzheimer's Disease Neuroimaging Initiative. A deep learning model for early prediction of Alzheimer's disease dementia based on hippocampal magnetic resonance imaging data. *Alzheimer's & Dementia*. 15(8) (2019), pp.1059-1070.
29. G. Mirzaei and H. Adeli. Machine learning techniques for diagnosis of Alzheimer's disease, mild cognitive disorder, and other types of dementia. *Biomedical Signal Processing and Control*. 72 (2022), p.103293.
30. N. Mammone, F.C. Ieracitano, H. Adeli and F.C. Morabito. Permutation Jaccard Distance-based Hierarchical Clustering to estimate EEG network density modifications in MCI subjects. *IEEE Transactions on Neural Networks and Learning Systems* (2018).
31. J.P. Amezquita-Sanchez, N. Mammone, M.C. Morabito, S. Marino and H. Adeli. A Novel Methodology for Automated Differential Diagnosis of Mild Cognitive Impairment and the Alzheimer's disease using EEG signals. *Journal of Neuroscience Methods*. 322 (2019), pp.88-95.
32. J.P. Amezquita-Sanchez, N. Mammone, F.C. Morabito and H. Adeli. A New Dispersion Entropy and Fuzzy Logic System-based Methodology for Automated Classification of Dementia Stages using Electroencephalograms. *Clinical Neurology and Neurosurgery*. 201 (2021), p.106446.
33. M. Ahmadlou, A. Adeli, R. Bajo and H. Adeli. Complexity of Functional Connectivity Networks in Mild Cognitive Impairment Patients during a Working Memory Task. *Clinical Neurophysiology*. 125:4 (2014), pp.694-702.
34. J. DelEtoile and H. Adeli. Graph theory and brain connectivity in Alzheimer's disease. *The Neuroscientist.* 23(6) (2017), pp.616-626.
35. A. Stamoulakatos, J. Cardona, C. Michie, I. Andonovic, P. Lazaridis, X. Bellekens, R. Atkinson, M.M. Hossain and C. Tachtatzis. A comparison of the performance of 2D and 3D convolutional neural networks for subsea survey video classification. Proceedings of OCEANS 2021, San Diego, CA, USA, 20–23 September 2021, IEEE, pp. 1–10, doi:10.23919/OCEANS44145.2021.9706125.
36. J. N. Kather, A. T. Pearson, N. Halama, D. Jäger, J. Krause, S.H. Loosen, A. Marx, P. Boor, F. Tacke, U.P. Neumann and H.I. Grabsch, Deep learning can predict microsatellite instability directly from histology in gastrointestinal cancer. *Nature medicine*, 25(7) (2019), pp.1054-1056.
37. B. N. Narayanan, R. Ali and R. C. Hardie. Performance analysis of machine learning and deep learning architectures for malaria detection on cell images. *In Applications of Machine Learning.* International Society for Optics and Photonics (SPIE). Vol. 11139 (2019), 111390W, pp. 240–247.

38. M. Sezgin and B. Sankur, Survey over image thresholding techniques and quantitative performance evaluation. *Journal of Electronic imaging*, *13*(1), (2004), pp.146-165.
39. D. Kaur and Y. Kaur, Various image segmentation techniques: a review. *International Journal of Computer Science and Mobile Computing*, *3*(5), (2014) pp.809-814.
40. Y. Lu, T. Jiang and Y. Zang, Region growing method for the analysis of functional MRI data. *NeuroImage*, *20*(1), (2003), pp.455-465.